The Riemann Sum Method for the Design of Sum-of-Cisoids Simulators for Rayleigh Fading Channels in Non-Isotropic Scattering Environments

Carlos A. Gutiérrez and Matthias Pätzold
Faculty of Engineering and Science, University of Agder
P.O. Box 509, 4898 Grimstad, Norway
Emails: cagutierrez@up.edu.mx, matthias.paetzold@uia.no

***Abstract*—In this paper, we introduce the Riemann sum method (RSM) as an effective tool for the design of sum-of-cisoids (SOC) simulators for narrowband mobile Rayleigh fading channels under non-isotropic scattering conditions. We show that the RSM results in an excellent approximation of the channel's autocorrelation function (ACF). Furthermore, we compare the performance of the RSM with that of the generalized method of equal areas (GMEA) and L_p-norm method (LPNM), which were until now the only methods available for the design of SOC simulators for non-isotropic scattering channels. The obtained results indicate that the RSM is better suited than the GMEA and the LPNM to approximate the channel's ACF, whereas the latter two methods provide better results regarding the emulation of the envelope distribution. Owing to its simplicity and good performance, the RSM can be used to design flexible simulation platforms for the analysis of mobile communication systems operating in non-isotropic scattering environments.**

***Keywords*—Channel simulators, mobile communications, non-isotropic scattering, Rayleigh fading channels, sum-of-cisoids, sum-of-sinusoids.**

I. Introduction

Simulation models having the ability to reproduce the statistical properties of non-isotropic scattering channels are highly desirable for the software-assisted performance analysis of modern mobile communication systems. They are important, for example, to study the channel capacity [1] and the bit error rate performance [2] in the realistic scenario where the Doppler power spectrum of the channel is asymmetrical [3].

It has been shown in a number of papers, e.g., [1], [4]–[6], that the simulation of non-isotropic scattering channels can efficiently be performed by means of a finite sum of complex sinusoids (cisoids). Sum-of-cisoids (SOC) models are closely related to the electromagnetic plane-wave propagation model [7]. They provide an excellent basis not only for enabling the simulation of narrowband single-input single-output (SISO) channels [5], but also for the simulation of wideband multiple-input multiple-output (MIMO) channels [8]. Currently, there exist only two parameter computation methods suitable for the design of SOC simulators for non-isotropic scattering channels, namely the L_p-norm method (LPNM) [4] and the generalized method of equal areas (GMEA) [5], [9]. Both methods produce good results regarding the emulation of the channel's statistics [4]–[6]. Nevertheless, the LPNM relies upon numerical optimization techniques that make the determination of the model parameters a time-consuming task. In contrast to this, the GMEA requires a comparatively large number of cisoids to properly emulate the channel's correlation properties [5]. The development of new methods, under the constraint of simplicity and accuracy, is therefore desirable to facilitate the performance analysis of modern and forthcoming mobile wireless communication systems.

In this paper, we introduce a simple and effective method for the design of SOC simulators for mobile Rayleigh fading channels under non-isotropic scattering conditions. The proposed method, which is based on a Riemann sum approximation of the channel's autocorrelation function (ACF), is presented here in the context of SISO channels. Its extension to the design of MIMO channel simulators is straightforward. We evaluate the performance of the Riemann sum method (RSM) with respect to its accuracy for emulating the ACF and the envelope distribution of the channel. What is more, we compare the performance of the RSM with that of the GMEA and the LPNM. Without loss of generality, we assume for our investigations that the angles of arrival (AOA) of the channel's multipath components are Laplacian distributed [10]. Our analysis shows that the RSM performs better than the LPNM and the GMEA regarding the emulation of the ACF, while the latter two methods are more precise concerning the approximation of the envelope distribution.

The rest of the paper is organized as follows. Sections II and III review the characteristics of the reference channel model and the SOC simulation model, respectively. Section IV introduces the RSM. Its performance is evaluated in Section V. Finally, our conclusions are given in Section VI.

II. The Reference Model

A. The Narrowband Rayleigh Fading Channel Model

We model the frequency-non-selective mobile fading channel in the equivalent complex baseband by a stationary zero-mean complex Gaussian process[1] $\boldsymbol{\mu}(t)$, which characterizes the complex channel gain in a two-dimensional small-scale

[1]Throughout the paper, we will make use of bold symbols and letters to denote random variables and stochastic processes, whereas we will employ normal symbols and letters for constants and deterministic processes.

9781-4244-3941-6/09/$25.00

propagation environment. On the basis of the central limit theorem [11, pp. 281-290] and following the scattering propagation model in [12, Sec. 1.1], we can represent such a channel model in terms of an infinite series of scattered azimuthal plane waves as follows

$$\boldsymbol{\mu}(t) \quad = \quad \lim_{N\to\infty} \sum_{n=1}^{N} \boldsymbol{c}_n e^{j(2\pi \boldsymbol{f}_n t + \boldsymbol{\theta}_n)} \tag{1}$$

where the nth plane wave is characterized by a cisoid with a random gain $\boldsymbol{c}_n$, a random phase $\boldsymbol{\theta}_n$, and a random Doppler frequency $\boldsymbol{f}_n$. The phases $\boldsymbol{\theta}_n$ are defined as independent and identically distributed (i.i.d.) random variables, each having a uniform distribution over $[-\pi, \pi)$. The gains $\boldsymbol{c}_n$ are given such that $E\{\boldsymbol{c}_n^2\} = \sigma_{\boldsymbol{\mu}}^2/N$ for $n = 1, 2, \ldots, N$, where $\sigma_{\boldsymbol{\mu}}^2$ is the variance of the complex Gaussian process $\boldsymbol{\mu}(t)$. The operator $E\{\cdot\}$ denotes statistical expectation. In turn, the Doppler frequencies $\boldsymbol{f}_n$ are defined as

$$\boldsymbol{f}_n \quad \triangleq \quad f_{\max} \cos(\boldsymbol{\alpha}_n), \quad \forall n = 1, 2, \ldots, N \tag{2}$$

where $\boldsymbol{\alpha}_n$ is the random AOA of the nth incoming wave, and $f_{\max}$ stands for the maximum Doppler frequency. The AOAs $\boldsymbol{\alpha}_n$ introduced above are assumed to be i.i.d. random variables characterized by a given probability density function (PDF) $p_{\boldsymbol{\alpha}}(\alpha)$, $\alpha \in [-\pi, \pi)$. The gains $\boldsymbol{c}_n$, phases $\boldsymbol{\theta}_n$, and AOAs $\boldsymbol{\alpha}_n$ are considered as being mutually independent.

The complex Gaussian process $\boldsymbol{\mu}(t)$, which acts in this paper as a reference channel model, can be characterized by its ACF $r_{\boldsymbol{\mu}\boldsymbol{\mu}}(\tau) \triangleq E\{\boldsymbol{\mu}^*(t)\boldsymbol{\mu}(t+\tau)\}$. The notation $(\cdot)^*$ indicates complex conjugation. One can easily verify that

$$r_{\boldsymbol{\mu}\boldsymbol{\mu}}(\tau) \quad = \quad 2\sigma_{\boldsymbol{\mu}}^2 \int_0^{\pi} g_{\boldsymbol{\alpha}}(\alpha)\, e^{j2\pi f_{\max} \cos(\alpha)\tau} d\alpha \tag{3}$$

where $g_{\boldsymbol{\alpha}}(\alpha) \triangleq [p_{\boldsymbol{\alpha}}(\alpha) + p_{\boldsymbol{\alpha}}(-\alpha)]/2$ is the even part of the PDF of $\boldsymbol{\alpha}$. Concerning the distribution of the channel's envelope $\boldsymbol{\zeta}(t) \triangleq |\boldsymbol{\mu}(t)|$, it can be shown that irrespective of the correlation properties of $\boldsymbol{\mu}(t)$, the PDF $p_{\boldsymbol{\zeta}}(z)$ of $\boldsymbol{\zeta}(t)$ is equal to [13, Sec. 6.1.1.1], [14]

$$p_{\boldsymbol{\zeta}}(z) \quad = \quad \frac{2z}{\sigma_{\boldsymbol{\mu}}^2} \cdot e^{-\frac{z^2}{\sigma_{\boldsymbol{\mu}}^2}}, \qquad z \geq 0 \tag{4}$$

which is known as the Rayleigh distribution [11, p. 113]. In addition, one can show that the PDF $p_{\boldsymbol{\phi}}(\theta)$ of the channel's phase $\boldsymbol{\phi}(t) \triangleq \arg\{\boldsymbol{\mu}(t)\}$ is given as [13, Sec. 6.1.1.1]

$$p_{\boldsymbol{\phi}}(\theta) \quad = \quad \frac{1}{2\pi}, \qquad \phi \in [-\pi, \pi). \tag{5}$$

B. The Laplacian PDF of the AOA and the Associated ACF

In order to demonstrate the performance of the RSM, it will be necessary to specify a concrete PDF for the random AOAs $\boldsymbol{\alpha}_n$. With this in mind, we suppose that $\boldsymbol{\alpha}_n$ follows the Laplacian distribution, which was first proposed in [10]. There, the authors demonstrated the goodness of fit of such a distribution by direct comparison with measured data collected in outdoor environments.

The Laplacian PDF of the AOA has the form [10]

$$p_{\boldsymbol{\alpha}}^{\mathrm{LA}}(\alpha) \quad = \quad \frac{1}{c_s} e^{-|\alpha|\frac{\sqrt{2}}{\sigma_s}}, \quad \alpha \in [-\pi, \pi) \tag{6}$$

where the parameter $\sigma_s > 0$ controls the angular spread, and

$$c_s = \sigma_s \sqrt{2} \left[1 - e^{-\pi \frac{\sqrt{2}}{\sigma_s}}\right] \tag{7}$$

is a normalization quantity that guarantees $\int_{-\infty}^{\infty} p_{\boldsymbol{\alpha}}^{\mathrm{LA}}(\alpha) d\alpha = 1$. Notice that $p_{\boldsymbol{\alpha}}^{\mathrm{LA}}(\alpha)$ is an even function, meaning that $g_{\boldsymbol{\alpha}}^{\mathrm{LA}}(\alpha) = p_{\boldsymbol{\alpha}}^{\mathrm{LA}}(\alpha)$. The ACF of $\boldsymbol{\mu}(t)$ cannot be written in closed form when the channel's AOA statistics follows the Laplacian PDF. Consequently, one has to use numerical methods to evaluate

$$r_{\boldsymbol{\mu}\boldsymbol{\mu}}^{\mathrm{LA}}(\tau) \quad = \quad \frac{2\sigma_{\boldsymbol{\mu}}^2}{c_s} \int_0^{\pi} e^{j2\pi f_{\max} \cos(\alpha)\tau - \alpha\frac{\sqrt{2}}{\sigma_s}} d\alpha. \tag{8}$$

The numerical integration of (8) does not pose any problems, as modern computers can accomplish the task easily.

III. The SOC-Based Simulation Model

One may observe from (1) that a hardware/software realization of the mobile fading channel described by $\boldsymbol{\mu}(t)$ is not possible, since it requires the implementation of a sum of an infinite number of cisoids. Fortunately, most of the statistical properties of $\boldsymbol{\mu}(t)$ relevant for system performance analysis—such as the correlation properties, spectral characteristics, and the first-order distributions of the envelope and phase—can satisfactorily be approximated by a simulation model described by a finite SOC. In this paper, we will perform such a task by considering a narrowband stochastic SOC simulation model with constant gains $\hat{c}_n$, constant Doppler frequencies $\hat{f}_n$, and random phases $\hat{\boldsymbol{\theta}}_n$. The stochastic SOC model can be represented by a random process $\hat{\boldsymbol{\mu}}(t)$ of the form

$$\hat{\boldsymbol{\mu}}(t) \quad = \quad \sum_{n=1}^{N} \hat{c}_n e^{j(2\pi \hat{f}_n t + \hat{\boldsymbol{\theta}}_n)}. \tag{9}$$

For the simulation of the reference model, we will consider the phases $\hat{\boldsymbol{\theta}}_n$ in (9) as being mutually independent and uniformly distributed over $[-\pi, \pi)$. In addition, we impose the condition $\sum_{n=1}^{N} \hat{c}_n^2 = \sigma_{\boldsymbol{\mu}}^2$ on the set of gains $\{\hat{c}_n\}_{n=1}^{N}$ and define the Doppler frequencies $\hat{f}_n$ as

$$\hat{f}_n \quad \triangleq \quad f_{\max} \cos(\hat{\alpha}_n), \quad \forall n = 1, 2, \ldots, N \tag{10}$$

where $\hat{\alpha}_n \in [-\pi, \pi)$. Under these conditions, one can show that $\hat{\boldsymbol{\mu}}(t)$ is a wide-sense stationary (WSS) process with mean zero, variance equal to $\sigma_{\boldsymbol{\mu}}^2$, and ACF

$$\begin{aligned} r_{\hat{\boldsymbol{\mu}}\hat{\boldsymbol{\mu}}}(\tau) \quad &\triangleq \quad E\{\hat{\boldsymbol{\mu}}^*(t)\hat{\boldsymbol{\mu}}(t+\tau)\} \\ &= \quad \sum_{n=1}^{N} \hat{c}_n^2 e^{j2\pi f_{\max} \cos(\hat{\alpha}_n)\tau}. \end{aligned} \tag{11}$$

Regarding the distribution of the envelope $\hat{\boldsymbol{\zeta}}(t) \triangleq |\hat{\boldsymbol{\mu}}(t)|$ of $\hat{\boldsymbol{\mu}}(t)$, it has recently been shown in [15] that the PDF $p_{\hat{\boldsymbol{\zeta}}}(z)$

of $\hat{\boldsymbol{\zeta}}(t)$ equals

$$p_{\hat{\boldsymbol{\zeta}}}(z) = z(2\pi)^2 \int_0^\infty \left[\prod_{n=1}^{N} J_0(2\pi|\hat{c}_n|x)\right] J_0(2\pi z x)x\,dx \qquad (12)$$

for $z \geq 0$. Investigations in [15] indicate that $p_{\hat{\boldsymbol{\zeta}}}(z)$ is in good agreement with the Rayleigh PDF for values of N as small as ten if $\hat{c}_n = \sigma_{\boldsymbol{\mu}}/\sqrt{N}$. With respect to the PDF $p_{\hat{\boldsymbol{\phi}}}(\hat{\theta})$ of the phase $\hat{\boldsymbol{\phi}}(t) \triangleq \arg\{\hat{\boldsymbol{\mu}}(t)\}$ of $\hat{\boldsymbol{\mu}}(t)$, it is also shown in [15] that

$$p_{\hat{\boldsymbol{\phi}}}(\hat{\theta}) \;=\; \frac{1}{2\pi}, \quad \hat{\theta} \in [-\pi, \pi). \qquad (13)$$

Interestingly, the PDF of $\hat{\boldsymbol{\phi}}(t)$ is not influenced by any of the SOC model parameters, not even by N. Without going into details, we observe that the stochastic SOC simulator described by $\hat{\boldsymbol{\mu}}(t)$ is mean-ergodic and autocorrelation-ergodic on condition that the Doppler frequencies $\hat{f}_n$ are specified such that $\hat{f}_n \neq 0\ \forall n$ and $\hat{f}_n \neq \hat{f}_m$, $n \neq m$. We refer the reader to [9] for further information in this respect.

IV. The Riemann Sum Method

Once the structure of the stochastic SOC simulation model has been defined, the problem consists in finding values for the model parameters that allow for a proper emulation of the statistics of the reference model. The problem lies basically in finding proper values for the gains $\hat{c}_n$ and Doppler frequencies $\hat{f}_n$ of the simulator, as the phases $\hat{\boldsymbol{\theta}}_n$ have no influence on the ACF $r_{\hat{\boldsymbol{\mu}}\hat{\boldsymbol{\mu}}}(\tau)$ in (11), nor on the PDFs $p_{\hat{\boldsymbol{\zeta}}}(z)$ and $p_{\hat{\boldsymbol{\phi}}}(\hat{\theta})$ in (12) and (13), respectively. A new solution to this problem is provided by the following RSM.

A. Basic Approach

We assume that the PDF $p_{\boldsymbol{\alpha}}(\alpha)$ of the AOAs $\boldsymbol{\alpha}_n$ contains no singularities, so that one can regard the integral in (3) as being a proper integral. Upon this assumption, $r_{\boldsymbol{\mu}\boldsymbol{\mu}}(\tau)$ can be written as a midpoint Riemann sum of the form

$$\begin{aligned} r_{\boldsymbol{\mu}\boldsymbol{\mu}}(\tau) \;&=\; \lim_{N\to\infty} \frac{2\pi\sigma_{\boldsymbol{\mu}}^2}{N} \sum_{n=1}^{N} g_{\boldsymbol{\alpha}}\Big(\frac{\pi}{N}\Big[n-\frac{1}{2}\Big]\Big) \\ &\quad \cdot \exp\left\{j2\pi f_{\max}\cos\Big(\frac{\pi}{N}\Big[n-\frac{1}{2}\Big]\Big)\tau\right\}. \qquad (14) \end{aligned}$$

If we drop the limit from the equation above, then we may presume that

$$\begin{aligned} r_{\boldsymbol{\mu}\boldsymbol{\mu}}(\tau) \;&\approx\; \frac{2\pi\sigma_{\boldsymbol{\mu}}^2}{N} \sum_{n=1}^{N} g_{\boldsymbol{\alpha}}\Big(\frac{\pi}{N}\Big[n-\frac{1}{2}\Big]\Big) \\ &\quad \cdot \exp\left\{j2\pi f_{\max}\cos\Big(\frac{\pi}{N}\Big[n-\frac{1}{2}\Big]\Big)\tau\right\}. \qquad (15) \end{aligned}$$

A comparison of (15) and (11) suggests that the ACF $r_{\hat{\boldsymbol{\mu}}\hat{\boldsymbol{\mu}}}(\tau)$ of $\hat{\boldsymbol{\mu}}(t)$ will render a good approximation to $r_{\boldsymbol{\mu}\boldsymbol{\mu}}(\tau)$ if we choose:

$$\hat{\alpha}_n \;=\; \frac{\pi}{N}\left(n-\frac{1}{2}\right) \qquad (16)$$

$$\hat{c}_n \;=\; \sigma_{\boldsymbol{\mu}}\sqrt{\frac{g_{\boldsymbol{\alpha}}(\hat{\alpha}_n)}{\sum_{m=1}^{N} g_{\boldsymbol{\alpha}}(\hat{\alpha}_m)}} \qquad (17)$$

for $n = 1, 2, \ldots, N$. Notice that the gains in (17) have been normalized to ensure that $\sum_{n=1}^{N} \hat{c}_n^2 = \sigma_{\boldsymbol{\mu}}^2$. The methodology given by (16) and (17) establishes a parameter computation method that we will refer to as the basic RSM (BRSM). It is worth mentioning that the idea behind the BRSM has recently been applied in [16] to simulate mobile MIMO Rayleigh fading channels, yielding remarkable results concerning the emulation of the spatial cross-correlation function and the temporal ACF.

From experiments, we have observed that irrespective of the AOA statistics, the BRSM provides an excellent approximation to the ACF of $\boldsymbol{\mu}(t)$ for $\tau \in \big[-\frac{N}{4f_{\max}}, \frac{N}{4f_{\max}}\big]$. Nevertheless, our experiments have also revealed that this method performs poorly regarding the emulation of the envelope distribution of $\boldsymbol{\mu}(t)$ if the angular spread is small, i.e., if the scattering is highly non-isotropic. Under such circumstances, there is a large difference between the gains $\hat{c}_n$ of the cisoids. Even though this characteristic does not entail any problems for the emulation of $r_{\boldsymbol{\mu}\boldsymbol{\mu}}(\tau)$, it does affect the ability of $\hat{\boldsymbol{\mu}}(t)$ for approximating the Rayleigh PDF, since the envelope distribution of $\hat{\boldsymbol{\mu}}(t)$ is heavily influenced by the gains $\hat{c}_n$ [see (12)]. The best fitting of $p_{\hat{\boldsymbol{\zeta}}}(z)$ against the Rayleigh distribution is obtained if all gains $\hat{c}_n$ are equal to $\hat{c}_n = \sigma_{\boldsymbol{\mu}}/\sqrt{N}$ [15].

B. Improved Approach

To overcome the aforementioned problem, we will present in what follows an improved version of the BRSM. To that end, we will assume that the PDF of the AOA is defined in such a way that its even part has at most one maximum in $[0, \pi)$. Thereby, for any given threshold $\gamma \in \big(0, \sup\{g_{\boldsymbol{\alpha}}(\alpha)\}_{\alpha\in[0,\pi)}\big)$, where $\sup\{\cdot\}$ denotes the supremum, we can identify one and only one subinterval $\mathcal{I}_U$ in $[0, \pi)$ satisfying

$$g_{\boldsymbol{\alpha}}(\alpha) \;>\; \gamma, \qquad \forall\alpha \in \mathcal{I}_U \qquad (18)$$

implying that $g_{\boldsymbol{\alpha}}(\alpha)$ is above the threshold only within $\mathcal{I}_U$. If the threshold is chosen low, so that $g_{\boldsymbol{\alpha}}(\alpha) \approx 0\ \forall\alpha \notin \mathcal{I}_U$, then one can state that

$$r_{\boldsymbol{\mu}\boldsymbol{\mu}}(\tau) \approx \sigma_{\boldsymbol{\mu}}^2 \int_{\alpha\in\mathcal{I}_U} g_{\boldsymbol{\alpha}}(\alpha)\exp\{j2\pi f_{\max}\cos(\alpha)\tau\}d\alpha. \qquad (19)$$

In such a case, it makes sense to compute the gains $\hat{c}_n$ and the AOAs $\hat{\alpha}_n$ of the stochastic SOC model by taking into account only the subinterval $\mathcal{I}_U$. Following this reasoning, we will redefine the AOAs $\hat{\alpha}_n$ as follows

$$\hat{\alpha}_n \;=\; \alpha_\ell + \frac{\alpha_u - \alpha_\ell}{N}\left(n-\frac{1}{2}\right), \quad \alpha_u > \alpha_\ell \qquad (20)$$

for $n = 1, 2, \ldots, N$, where α_ℓ and α_u designate the lower and the upper boundaries of $\mathcal{I}_U$. The methodology resulting in (17) and (20) constitutes the RSM.

Choosing a proper value for the threshold γ is clearly the critical step in the RSM. When setting the threshold, one has to be aware of the fact that the method will be affected by the same problems as the BRSM if γ is too low. On the other hand, if γ is large, then the RSM will become more precise regarding

the approximation of the envelope distribution of $\boldsymbol{\mu}(t)$, but it will loose accuracy with respect to the approximation of $r_{\boldsymbol{\mu}\boldsymbol{\mu}}(\tau)$. While determining an optimal value for γ is not a trivial issue, we have found from practice that setting $\gamma = 1 \times 10^{-3}$ results in case of the Laplacian distribution in a good approximation to $r_{\boldsymbol{\mu}\boldsymbol{\mu}}(\tau)$ and $p_{\boldsymbol{\zeta}}(z)$, as will be shown in the following section.

V. Performance Analysis

A. Simulation Set-Up and Considerations

In what follows, we present a performance comparison among the RSM, the GMEA [5], [9], and the LPNM [4] in terms of the emulation of the ACF and the envelope distribution of the reference model. To that end, we assume that the channel's AOA statistics follows the Laplacian distribution with $\sigma_s \in \{0.5, 1, 5\}$. Such values of σ_s are representative of non-isotropic scattering conditions ranging from moderated ($\sigma_s = 5$) to severe ($\sigma_s = 0.5$).

In the case of the RSM, the boundaries of the subinterval $\mathcal{I}_U = [\alpha_\ell, \alpha_u)$ are to be found by identifying the points in $[0, \pi)$ at which the function $g_{\boldsymbol{\alpha}}(\alpha)$ crosses the threshold γ from up to down (corresponding to α_u) and/or from down to up (corresponding to α_ℓ). For the Laplacian distribution, the lower boundary α_ℓ of $\mathcal{I}_U$ is found to be equal to $\alpha_\ell = 0$, since $g^{\mathrm{LA}}_{\boldsymbol{\alpha}}(\alpha)$ is a monotonically decreasing function in $[0, \pi)$ and therefore no up-crossing is observed within that interval. In turn, the upper boundary α_u is found to be given by

$$\alpha_u \quad = \quad -\frac{\sigma_s}{\sqrt{2}} \ln(\gamma c_s) \tag{21}$$

which is the solution of $g^{\mathrm{LA}}_{\boldsymbol{\alpha}}(\alpha) - \gamma = 0$. If this equation has no solutions in $[0, \pi)$, then α_u is set to π. We have chosen $\gamma = 1 \times 10^{-3}$ to carry out our simulations.

In the case of the GMEA, the gains $\hat{c}_n$ are given by [5], [9]

$$\hat{c}_n \quad = \quad \frac{\sigma_{\boldsymbol{\mu}}}{\sqrt{N}}, \quad n = 1, 2, \ldots, N \tag{22}$$

whereas the Doppler frequencies $\hat{f}_n$ are to be found by solving the equation

$$\int_0^{\hat{\alpha}_n} g^{\mathrm{LA}}_{\boldsymbol{\alpha}}(\alpha)\, d\alpha - \frac{1}{2N}\left(n - \frac{1}{2}\right) = 0 \tag{23}$$

for $n = 1, 2, \ldots, N$. It can easily be verified that the solution of (23) is given by

$$\hat{f}_n = f_{\max} \cos\left(\frac{\sigma_s}{\sqrt{2}} \ln\left(1 - \frac{c_s}{\sqrt{2} N \sigma_s}\left[n - \frac{1}{2}\right]\right)\right). \tag{24}$$

The LPNM, as presented in [4], also defines the gains of $\hat{\boldsymbol{\mu}}(t)$ as in (22), but it requires the parameters $\hat{f}_n$ to be computed by minimizing the L_p-norm

$$\epsilon^{(p)}_{r_{\boldsymbol{\mu}\boldsymbol{\mu}}} \quad \triangleq \quad \left\{\frac{1}{\tau_{\max}} \int_0^{\tau_{\max}} \left| r_{\boldsymbol{\mu}\boldsymbol{\mu}}(\tau) - r_{\hat{\boldsymbol{\mu}}\hat{\boldsymbol{\mu}}}(\tau)\right|^p d\tau\right\}^{1/p} \tag{25}$$

where p is a positive integer and $\tau_{\max} > 0$ determines the length of the interval $[0, \tau_{\max}]$ inside of which the approximation $r_{\boldsymbol{\mu}\boldsymbol{\mu}}(\tau) \approx r_{\hat{\boldsymbol{\mu}}\hat{\boldsymbol{\mu}}}(\tau)$ is of interest. The minimization of $\epsilon^{(p)}_{r_{\boldsymbol{\mu}\boldsymbol{\mu}}}$ has to be done by applying a numerical optimization algorithm, e.g., that described in [17], which can efficiently be implemented by using the `fminsearch` function of MATLAB®. We have employed the Doppler frequencies defined by the GMEA as initial values to minimize (25). In addition, we set $p = 2$ and $\tau_{\max} = N/(4 f_{\max})$.

B. Emulation of the ACF

The absolute value of the ACF of the reference model, $|r^{\mathrm{LA}}_{\boldsymbol{\mu}\boldsymbol{\mu}}(\tau)|$ [see (8)], is plotted in Fig. 1 against the absolute value of the ACF of the simulation model, $|r_{\hat{\boldsymbol{\mu}}\hat{\boldsymbol{\mu}}}(\tau)|$ [see (11)], by applying each of the three methods under consideration with $N = 20$. One can observe from the graphs depicted in Fig. 1 that the RSM outperforms by far the LPNM and the GMEA. In fact, in the case of the RSM, no differences between $|r^{\mathrm{LA}}_{\boldsymbol{\mu}\boldsymbol{\mu}}(\tau)|$ and $|r_{\hat{\boldsymbol{\mu}}\hat{\boldsymbol{\mu}}}(\tau)|$ are visible within the interval $[0, 5/f_{\max}]$. However, the performance of the LPNM and the GMEA is reasonably good. We can see in Fig. 1 that the LPNM yields a better approximation to $|r^{\mathrm{LA}}_{\boldsymbol{\mu}\boldsymbol{\mu}}(\tau)|$ than the GMEA, as was to be expected. Nevertheless, the graphs of $|r_{\hat{\boldsymbol{\mu}}\hat{\boldsymbol{\mu}}}(\tau)|$ produced by the GMEA are in general closer to those of $|r^{\mathrm{LA}}_{\boldsymbol{\mu}\boldsymbol{\mu}}(\tau)|$ at the vicinities of the origin ($\tau = 0$) than the graphs obtained by using the LPNM.

C. Emulation of the Envelope Distribution

Figures 2 and 3 show a comparison between the envelope PDF of the reference model, $p_{\boldsymbol{\zeta}}(z)$ [see (4)], and the PDF of the envelope of $\hat{\boldsymbol{\mu}}(t)$, $p_{\hat{\boldsymbol{\zeta}}}(z)$ [see (12)]. Again, the depicted graphs of $p_{\hat{\boldsymbol{\zeta}}}(z)$ were generated by considering $N = 20$ and $\sigma^2_{\boldsymbol{\mu}} = 1$. We observe that the evaluation of (12) results in exactly the same PDF $p_{\hat{\boldsymbol{\zeta}}}(z)$ for the GMEA and the LPNM. This is due to the fact that the solution given in (12) for $p_{\hat{\boldsymbol{\zeta}}}(z)$ is solely influenced by the set of gains $\{\hat{c}_n\}$, and both the GMEA and the LPNM define the gains of $\hat{\boldsymbol{\mu}}(t)$ in the same way [cf. (22)]. Concerning the methods' performance, the results presented in Figs. 2 and 3 show clearly that the LPNM and the GMEA are better suited than the RSM to approximate the distribution of $\boldsymbol{\zeta}(t)$. In fact, we can see in Fig. 2 that the graphs of $p_{\hat{\boldsymbol{\zeta}}}(z)$ line up almost perfectly with the curve described by $p_{\boldsymbol{\zeta}}(z)$. In contrast, the curves of $p_{\hat{\boldsymbol{\zeta}}}(z)$ depicted in Fig. 3 for the RSM exhibit some deviations from $p_{\boldsymbol{\zeta}}(z)$ that become more pronounced the smaller the value of σ_s is, that is, the more non-isotropic the scattering becomes. Despite of such deviations, the RSM provided a quite good approximation to $p_{\boldsymbol{\zeta}}(z)$.

VI. Summary and Conclusions

In this paper, we introduced the RSM as an effective parameter computation method enabling the design of SOC simulation models for narrowband mobile Rayleigh fading channels under non-isotropic scattering conditions. We evaluated the performance of the RSM in terms of the approximation of the ACF and envelope distribution of the channel. Results

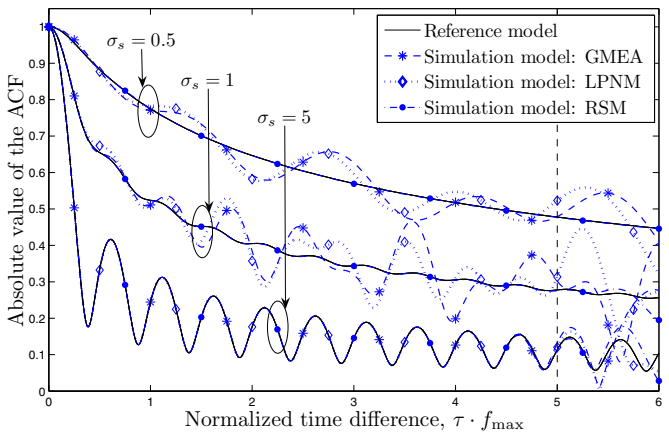

Fig. 1. Comparison among the GMEA, the LPNM, and the RSM in terms of the emulation of the reference model's ACF by considering the Laplacian PDF of the AOA with different values of the parameter σ_s ($N = 20$, $f_{\max} = 91$ Hz, $\sigma_{\boldsymbol{\mu}}^2 = 1$, $p = 2$, $\tau_{\max} = 5/f_{\max}$, $\gamma = 1 \times 10^{-3}$).

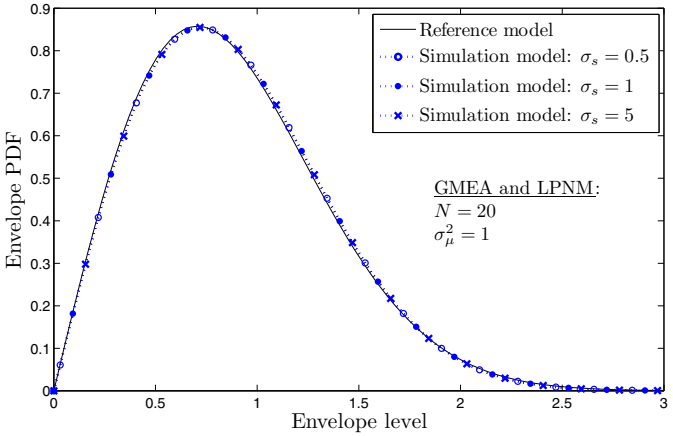

Fig. 2. Comparison between the envelope PDF of the reference model and the envelope PDF of the simulation model by applying the GMEA and the LPNM on the Laplacian PDF of the AOA with different values of the parameter σ_s ($f_{\max} = 91$ Hz, $p = 2$, and $\tau_{\max} = 5/f_{\max}$).

obtained by applying the GMEA and the LPNM were also reported in this paper and compared with those produced by the RSM. Our investigations indicate that the RSM is better suited than the LPNM and the GMEA to emulate the channel's correlation characteristics, whereas the LPNM and the GMEA are more precise than the RSM regarding the approximation of the Rayleigh PDF. In addition to its good performance, the simplicity of the RSM makes this method a suitable tool for the design of simulation platforms for the analysis of modern and forthcoming mobile communication systems.

REFERENCES

[1] M. Pätzold and B. O. Hogstad, "A space-time channel simulator for MIMO channels based on the geometrical one-ring scattering model," *Wirel. Commun. Mob. Comput.*, vol. 4, no. 7, pp. 727–737, Nov. 2004.

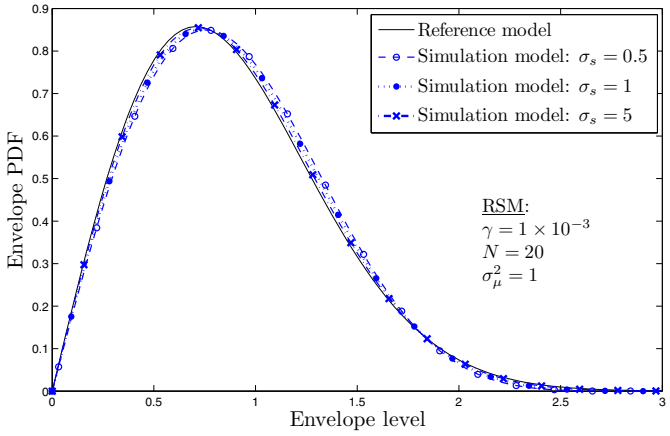

Fig. 3. Comparison between the envelope PDF of the reference model and the envelope PDF of the simulation model by applying the RSM on the Laplacian PDF of the AOA with different values of the parameter σ_s ($f_{\max} = 91$ Hz).

[2] S. A. Mitilineos, P. K. Varlamos, and C. N. Capsalis, "A simulation method for bit-error-rate-performance estimation for arbitrary angle of arrival channel models," *IEEE Antennas Propag. Mag.*, vol. 46, no. 2, pp. 158–163, Apr. 2004.

[3] X. Zhao, J. Kivinen, P. Vainikainen, and K. Skog, "Characterization of Doppler spectra for mobile communications at 5.3 GHz," *IEEE Trans. Veh. Technol.*, vol. 52, no. 1, pp. 14–23, Jan. 2003.

[4] M. Pätzold and N. Youssef, "Modelling and simulation of direction-selective and frequency-selective mobile radio channels," *Int. J. Electron. Commun.*, vol. AEÜ-55, no. 6, pp. 433–442, Nov. 2001.

[5] C. A. Gutiérrez and M. Pätzold, "Sum-of-sinusoids-based simulation of flat-fading wireless propagation channels under non-isotropic scattering conditions," in *Proc. 50th IEEE Global Communications Conference (Globecom 2007)*, Washington, DC, Nov. 2007, pp. 3842–3846.

[6] M. Pätzold, B. O. Hogstad, and N. Youssef, "Modeling, analysis, and simulation of MIMO mobile-to-mobile fading channels," *IEEE Trans. Wireless Commun.*, vol. 7, no. 2, pp. 510–520, Feb. 2008.

[7] W. R. Braun and U. Dersch, "A physical mobile radio channel model," *IEEE Trans. Veh. Technol.*, vol. 40, no. 2, pp. 472–482, May 1991.

[8] M. Pätzold and B. O. Hogstad, "A wideband MIMO channel model derived from the geometric elliptical scattering model," *Wirel. Commun. Mob. Comput.*, vol. 8, no. 5, pp. 597–605, Jun. 2008.

[9] C. A. Gutiérrez, *Channel Simulation Models for Mobile Broadband Communication Systems, Doctoral Dissertations at the University of Agder 16*. Kristiansand, Norway: University of Agder, 2009.

[10] K. I. Pedersen, P. E. Mogensen, and B. H. Fleury, "Power azimuth spectrum in outdoor environments," *IEE Electron. Lett.*, vol. 33, no. 18, pp. 1583–1584, Aug. 1997.

[11] A. Leon-Garcia, *Probability and Random Processes for Electrical Engineering*, 2nd ed. New York: Addison-Wesley, 1994.

[12] W. C. Jakes, *Microwave Mobile Communications*. Piscataway, NJ: IEEE Press, 1994.

[13] M. Pätzold, *Mobile Fading Channels*. Chichester, UK: John Wiley and Sons, 2002.

[14] T. Aulin, "A modified model for the fading signal at a mobile radio channel," *IEEE Trans. Veh. Technol.*, vol. 28, no. 3, pp. 182–203, Aug. 1979.

[15] M. Pätzold and B. Talha, "On the statistical properties of sum-of-cisoids-based mobile radio channel simulators," in *Proc. 10th Int. Symp. on Wireless Personal Multimedia Communications (WPMC'07)*, Jaipur, India, Dec. 2007.

[16] C. A. Gutiérrez and M. Cabrera-Bean, "Deterministic simulation of flat-fading MIMO wireless channels under non-isotropic scattering conditions," in *Proc. 17th IEEE Int. Symp. on Personal, Indoor, and Mobile Radio Communications (PIMRC'07)*, Athens, Greece, Sep. 2007.

[17] J. C. Lagarias, J. A. Reeds, M. H. Wright, and P. E. Wright, "Convergence properties of the Nelder–Mead simplex method in low dimensions," *SIAM Journal of Optimization*, vol. 9, no. 1, pp. 112–147, 1998.